On the performance of SOLD methods for convection–diffusion problems with interior layers

V. John

Universität des Saarlandes,
Fachbereich 6.1 – Mathematik,
Postfach 15 11 50,
66041 Saarbrücken, Germany
E-mail: john@math.uni-sb.de

P. Knobloch*

Charles University,
Faculty of Mathematics and Physics,
Department of Numerical Mathematics,
Sokolovská 83, 18675 Praha 8, Czech Republic
E-mail: knobloch@karlin.mff.cuni.cz
*Corresponding author

Abstract: Numerical solutions of convection–diffusion equations obtained using the Streamline–Upwind Petrov–Galerkin (SUPG) stabilisation typically possess spurious oscillations at layers. Spurious Oscillations at Layers Diminishing (SOLD) methods aim to suppress or at least diminish these oscillations without smearing the layers extensively. In the recent review by John and Knobloch (2007), numerical studies at convection–diffusion problems with constant convection whose solutions have boundary layers led to a pre-selection of the best available SOLD methods with respect to the two goals stated above. The behaviour of these methods is studied in this paper for a convection–diffusion problem with a non-constant convection field whose solution possesses an interior layer.

Keywords: convection–diffusion equations; streamline–upwind Petrov–Galerkin (SUPG) method; spurious oscillations at layers diminishing (SOLD) methods; interior layers.

Reference to this paper should be made as follows: John, V. and Knobloch, P. (2007) 'On the performance of SOLD methods for convection–diffusion problems with interior layers', *Int. J. Computing Science and Mathematics*, Vol. 1, Nos. 2/3/4, pp.245–258.

Biographical notes: Volker John is a Professor of Applied Mathematics at the University of the Saarland. He received his Diploma Degree in 1992 from the University of Halle-Wittenberg (Germany), his PhD Degree in 1997 and his habilitation in 2002 from the Otto-von-Guericke-University Magdeburg (Germany). In 2005 he moved to the University of the Saarland. His research interests include finite element methods in CFD, in particular for turbulent flows, convection-diffusion equations and coupled systems.

Petr Knobloch received his MS Degree from the Charles University in Prague (Czech Republic) in 1993 and his PhD Degree from the Otto-von-Guericke-University Magdeburg (Germany) in 1996. He is currently an Associate Professor at the Department of Numerical Mathematics of the Faculty of Mathematics and Physics at the Charles University in Prague. His research interests are the finite element method in general and numerical solution of fluid flow and singularly perturbed problems in particular.

1 Introduction

Scalar convection–diffusion equations

$$\begin{aligned} -\varepsilon\Delta u + \mathbf{b}\cdot\nabla u &= f \quad \text{in } \Omega, \\ u &= g_D \quad \text{on } \partial\Omega_D, \\ \varepsilon\frac{\partial u}{\partial \mathbf{n}} &= g_N \quad \text{on } \partial\Omega_N, \end{aligned} \tag{1}$$

describe the stationary distribution of a quantity u, like concentration or temperature, determined by the physical mechanisms of convection and diffusion. In equation (1), $\Omega \subset \mathbb{R}^d$, $d \in \{2, 3\}$, is a bounded domain with a polygonal or polyhedral boundary $\partial\Omega$ with subsets $\partial\Omega_D$ and $\partial\Omega_N$ satisfying $\partial\Omega = \partial\Omega_D \cup \partial\Omega_N$ and $\partial\Omega_D \cap \partial\Omega_N = \emptyset$. Further, $\varepsilon \in \mathbb{R}_+$ is a constant diffusion coefficient, $\mathbf{b} \in W^{1,\infty}(\Omega)^d$ is a given convection field satisfying the incompressibility condition $\nabla \cdot \mathbf{b} = 0$, $f \in L^2(\Omega)$ is an outer source of the quantity u, $\mathbf{n}$ is the outward unit normal vector to $\partial\Omega$, $g_D \in H^{1/2}(\partial\Omega_D)$ represents Dirichlet boundary conditions and $g_N \in H^{-1/2}(\partial\Omega_N)$ Neumann boundary conditions. The solution of equation (1) is sought in $H^1(\Omega)$.

The interesting case from the practical as well as from the numerical point of view is the convection-dominated one, i.e., $\varepsilon \ll \| \mathbf{b} \|_{L^\infty(\Omega)}$. In this case, the solution of equation (1) typically possesses layers. These are regions where the solution still is continuous but has very large gradients. The width of the layers is in general much smaller than the available mesh width in numerical simulations. Consequently, the layers cannot be resolved. It turns out that standard discretisation approaches, like the Galerkin Finite Element Method (FEM), even lead to solutions that are globally polluted by spurious (unphysical) oscillations.

A dramatical enhancement of the quality of numerical solutions is obtained with stabilised discretisations. In the context of FEM, there are several approaches like upwind techniques (Tabata, 1977), the Streamline–Upwind Petrov–Galerkin (SUPG) method (Brooks and Hughes, 1982), also called Streamline-Diffusion Finite Element Method (SDFEM), or the Galerkin/least-squares method (Hughes et al., 1989), see Roos et al. (1996) for an overview. The most popular one is probably the SUPG method, which will be also considered in this paper.

Applying the SUPG stabilisation, the numerical solutions capture the position of the layers in general quite well and the layers are not smeared. However, spurious oscillations of sometimes considerable magnitude usually appear at the layers. These oscillations are intolerable from the physical point of view since they describe,

for instance, negative concentrations. From the numerical point of view, these oscillations might lead to instabilities in the simulation of coupled systems which involve equations of form (1), for instance if, due to negative spurious oscillations, reactive terms of product form change locally their signs in coupled, non-linear reaction–convection–diffusion equations. Thus, there is an urgent need to remove these spurious oscillations, however, without smearing the layers extensively.

The development of numerical schemes for removing (or at least diminishing) the spurious oscillations of SUPG solutions of equation (1) started around two decades ago. Since then, a number of different approaches have been published, see, e.g., the recent review by John and Knobloch (2007). These schemes were called often *shock capturing methods* or *discontinuity capturing methods;* however, these names do not reflect their real purpose. Therefore, the name spurious oscillations at layers diminishing (SOLD) methods was introduced by John and Knobloch (2007) and this name will be used in this paper, too.

In the review paper by John and Knobloch (2007), numerical tests with constant convection fields and P_1 finite elements are presented to compare most of the published SOLD methods and to obtain a pre-selection of methods that should be studied in detail. The methods were evaluated by means of various criteria, which measure the amount of spurious oscillations and the smearing of the layers in the discrete solution. Thus, if we speak about 'best methods' in the present paper, we always mean with respect to those criteria (if we refer to John and Knobloch (2007)) or with respect to the criteria formulated below. We believe that this procedure is necessary before one should study the error of the discrete solution measured in various norms since such a study makes only sense for methods which substantially reduce the spurious oscillations without an extensive smearing of layers (other methods are not useful in applications). However, based on all our experiences, there is still no method fulfilling this requirement (save (Mizukami and Hughes, 1985) in special cases, see below) and therefore a study of approximation errors is not yet an issue. In our opinion, there are no relations between the measures for evaluating the size of the oscillations and norms in which the approximation error is bounded.

The aim of this paper is to present numerical studies for the best SOLD methods from John and Knobloch (2007) for a problem without boundary layers but with an interior layer created by a non-constant convection field. For such a problem, the localised spurious oscillations of the SUPG solution cannot be significantly influenced by the choice of the stabilisation parameter τ (see below) since the SUPG method does not contain any mechanism for stabilisation perpendicular to streamlines. Let us mention that we do not use layer-adapted meshes (like Bakhvalov or Shishkin type meshes) since our aim is to find methods that can be used in applications, which means in situations where the features of the solution (and hence a layer-adapted mesh) are not known a priori.

The plan of the paper is as follows. In the next section, we formulate the SUPG method and, in Section 3, we review SOLD methods, which were identified as the best ones by John and Knobloch (2007). Then, in Section 4, we present results of our numerical studies. In contrast to John and Knobloch (2007), the Q_1 finite element is used besides the P_1 finite element. The paper ends with our conclusions in Section 5.

2 SUPG method

The SUPG method adds an additional term to the Galerkin FEM to control the derivatives in streamline direction. Let the space $H^1(\Omega)$ in which the solution of equation (1) is sought be approximated by a conforming finite element subspace V_h defined on an admissible triangulation $\mathcal{T}_h$ (Ciarlet, 1991) with elements (mesh cells) K. We introduce a function $g_{D,h} \in V_h$ such that $g_{D,h} \mid_{\partial\Omega_D}$ approximates g_D. Further, we set $V_{0,h} = \{v \in V_h : v \mid_{\partial\Omega_D} = 0\}$. Then, the SUPG method reads as follows: Find $u_h \in V_h$ such that $u_h - g_{D,h} \in V_{0,h}$ and

$$\begin{aligned}(\varepsilon\nabla u_h, \nabla v_h) + (\mathbf{b}\cdot\nabla u_h, v_h) + \sum_{K\in\mathcal{T}_h} (R_h(u_h), \tau\mathbf{b}\cdot\nabla v_h)_K \\ = (f, v_h) + \int_{\partial\Omega_N} g_N v_h \, \mathrm{d}s \quad \forall\, v_h \in V_{0,h},\end{aligned} \tag{2}$$

where $(\cdot,\cdot)_K$ denotes the inner product in $L^2(K)$ or $L^2(K)^d$, $(\cdot,\cdot) = (\cdot,\cdot)_\Omega$,

$$R_h(u_h)|_K = -\varepsilon\Delta(u_h|_K) + (\mathbf{b}\cdot\nabla u_h - f)|_K$$

and $\tau \in L^\infty(\Omega)$ is a non-negative stabilisation parameter. There are several approaches for choosing τ, see John and Knobloch (2007), which lead asymptotically to optimal error estimates. However, they may lead to very different results for a concrete situation and the optimal choice of τ is an open question. We will use in the simulations presented in this paper the following definition:

$$\tau|_K(\mathbf{x}) = \frac{h_{K,\mathbf{b}}(\mathbf{x})}{2\,|\mathbf{b}(\mathbf{x})|}\xi(\mathrm{Pe}_K(\mathbf{x})) \tag{3}$$

with the local Péclet number

$$\mathrm{Pe}_K(\mathbf{x}) = \frac{|\mathbf{b}(\mathbf{x})|\, h_{K,\mathbf{b}}(\mathbf{x})}{2\varepsilon},$$

the upwind function $\xi(\alpha) = \coth(\alpha) - \alpha^{-1}$, $|\mathbf{b}(\mathbf{x})|$ the Euclidean norm of the convection vector in $\mathbf{x} \in K$ and $h_{K,b}(\mathbf{x})$ the diameter of the element K in the direction of $\mathbf{b}(\mathbf{x})$, see John and Knobloch (2007) for a detailed discussion of these choices.

3 SOLD methods

The most SOLD methods considered in the review by John and Knobloch (2007) are defined by adding an artificial diffusion term to the SUPG discretisation (2). The review by John and Knobloch (2007) categorises the available SOLD methods into the following classes:

- SOLD methods adding isotropic artificial diffusion
- SOLD methods adding crosswind artificial diffusion
- SOLD methods based on edge stabilisations
- SOLD methods that are not based on the SUPG method.

Note that the additional terms lead generally to non-linear discrete equations. Below, we formulate the SOLD method(s) from each class, which are the best ones according to the tests and criteria in John and Knobloch (2007) (and also according to further numerical studies we have performed).

SOLD methods adding isotropic artificial diffusion add the term

$$\sum_{K\in\mathcal{T}_h} (\tilde{\varepsilon}\nabla u_h, \nabla v_h)_K$$

to the left-hand side of equation (2). Among the schemes reviewed in John and Knobloch (2007), the best method of this type seems to be that one proposed by do Carmo and Galeão (1991) (dCG91) in which

$$\tilde{\varepsilon} = \tau \max\left\{0, \frac{|\mathbf{b}||R_h(u_h)|}{|\nabla u_h|} - \frac{|R_h(u_h)|^2}{|\nabla u_h|^2}\right\}$$

(we set $\tilde{\varepsilon} = 0$ if $\nabla u_h = 0$). Here, τ is the same as in equation (3).

SOLD methods adding crosswind diffusion introduce an extra term of the form

$$\sum_{K\in\mathcal{T}_h} (\tilde{\varepsilon}D\nabla u_h, \nabla v_h)_K$$

with

$$D = \begin{cases} I - \dfrac{\mathbf{b}\otimes\mathbf{b}}{|\mathbf{b}|^2} & \text{if } \mathbf{b} \neq \mathbf{0} \\ 0 & \text{else} \end{cases}$$

into the SUPG formulation (2). The best results in this class of SOLD methods in John and Knobloch (2007) were obtained with modifications proposed by John and Knobloch (2007) of a parameter suggested by Codina (1993) (C93) and of a parameter by Burman and Ern (2002) (BE02). The parameter of the method C93 is

$$\tilde{\varepsilon}|_K = \max\left\{0, C\frac{h_K |R_h(u_h)|}{2|\nabla u_h|} - \varepsilon\right\}$$

($\tilde{\varepsilon} = 0$ if $\nabla u_h = 0$), where C is a user-chosen parameter and h_K is the diameter of the element K. In the numerical studies in Section 4, the parameter $C = 0.6$ will be used, which is the same value as in John and Knobloch (2007). If $f = 0$ and $\Delta(u_h|_K) = 0$ for any $K \in \mathcal{T}_h$ (which will be the case in Section 4), the above definition of $\tilde{\varepsilon}$ is identical with the original method of Codina (1993). The parameter of BE02 has the form

$$\tilde{\varepsilon}|_K = \frac{\tau|\mathbf{b}|^2 |R_h(u_h)|}{|\mathbf{b}||\nabla u_h| + |R_h(u_h)|}.$$

Edge stabilisation methods for linear simplicial finite elements add to the left-hand side of equation (2) the term

$$\sum_{K\in\mathcal{T}_h} \int_{\partial K} \Psi_K(u_h)\operatorname{sign}\left(\frac{\partial u_h}{\partial \mathbf{t}_{\partial K}}\right)\frac{\partial v_h}{\partial \mathbf{t}_{\partial K}}\,\mathrm{d}s,$$

where $\mathbf{t}_{\partial K}$ is a tangential vector on the boundary ∂K of K. The best edge stabilisation method in the numerical studies of John and Knobloch (2007) was proposed by Burman and Ern (2005) (BE05). It has the parameter function

$$\Psi_K(u_h) = C\,|\,R(u_h)|_K\,|.$$

The same parameter $C = 5 \times 10^{-5}$ as in John and Knobloch (2007) was chosen for the numerical studies presented below.

From the approaches that do not rely on the SUPG method, we will consider an upwind scheme, which was developed by Mizukami and Hughes (1985) (MH85) and recently improved by Knobloch (2006). This upwind scheme is defined only for linear simplicial finite elements and is based on a rather involved geometrical construction, see Knobloch (2006) for details.

For further properties of the SOLD methods, we refer to John and Knobloch (2007).

4 Numerical studies

We will study (1) with $\Omega = (0, 1)^2$, $\partial\Omega_N = \{0\} \times (0, 1)$, $f = 0$ and $\mathbf{b}(x, y) = (-y, x)^T$. On the outflow boundary $\partial\Omega_N$, homogeneous conditions $g_N = 0$ are prescribed. The Dirichlet data are discontinuous

$$g_D(x,y) = \begin{cases} 1 & \text{if } (x,y) \in (1/3, 2/3) \times \{0\}, \\ 0 & \text{else on } \partial\Omega_D. \end{cases}$$

The discontinuous Dirichlet boundary condition on $(0, 1) \times \{0\}$ is transported counter-clockwise to the outflow boundary, see Figure 1. The width of the layers, for instance on the outflow boundary, depends on the size of ε. This example was already studied by Knopp et al. (2002). The solution u of the continuous problem does not belong to $H^1(\Omega)$ but, due to the positive diffusion, u is smooth in Ω. Moreover, it is easy to smooth g_D to a function from $H^{1/2}(\partial\Omega_D)$ (which leads to $u \in H^1(\Omega)$) in such a way that the numerical results presented in this paper do not change. We will study the cases of a moderate local Péclet number and of a high local Péclet number. Similarly as in John and Knobloch (2007), the SOLD methods will be evaluated only on measures for the amount of spurious oscillations and layer smearing. The results have been double checked with two different codes, one of them was MooNMD (John and Matthies, 2004).

Figure 1 Solution u for $\varepsilon = 10^{-4}$, blue (dark) part is zero, red (light) part is one

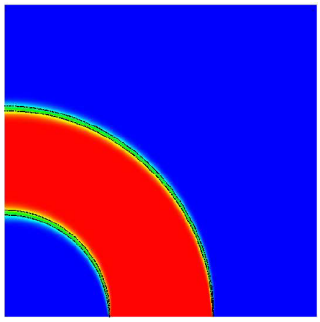

4.1 Moderate local mesh Péclet numbers

First, we will present computations for $\varepsilon = 10^{-4}$. For this diffusion parameter, we computed a reference solution with the Galerkin FEM (P_2 FEM, 16 785 409 degrees of freedom (dof), $h_K = \sqrt{2}/2048$), see Figure 2, which will be used to evaluate the SOLD methods.

Figure 2 Reference curve for $\varepsilon = 10^{-4}$ on the outflow boundary

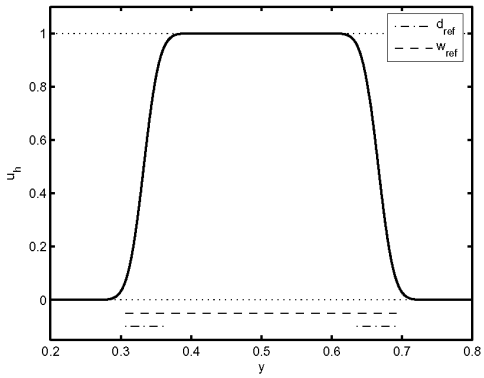

The initial regular grids and the unstructured triangular grid are presented in Figure 3. Refining the regular grids till the legs of the triangles or the edges of the squares have the length 1/32 leads to 1089 dof (including Dirichlet nodes). The unstructured grid (Grid 3) has 1244 nodes and was obtained using the anisotropic mesh adaptation technique of Dolejší (1998). The P_1 finite element was used on the simplicial grids (Grid 1–Grid 3) and the Q_1 finite element on the grid consisting of squares (Grid 4). The integrals in the discrete problem were evaluated using quadrature rules which are exact for polynomials of degree 8 (triangles) and 9 (squares).

Figure 3 The grids used in the computations: Grid 1, Grid 2, Grid 3 and Grid 4 (left to right, top to bottom). The structured grids are refined till the length of the legs of the triangles (edges of the squares) is 1/32 in the moderate local Péclet number case and 1/64 in the high local Péclet number case

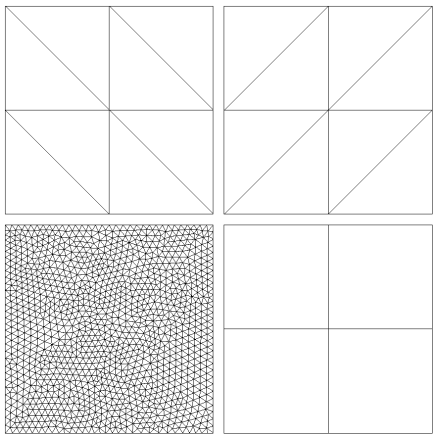

Since the convection field is not constant, the local mesh Péclet numbers vary in Ω. The lowest Péclet number is on all grids zero (at the corner $(0, 0)$). The largest Péclet number is around 150 on Grid 2, 240 on Grid 3 and about 300 on Grid 1 and Grid 4. Note that the local mesh Péclet numbers in the regions with the layers are smaller.

Let us denote by $\mathcal{N}_h$ the set of nodes of the triangulation $\mathcal{T}_h$. The measures for evaluating the numerical results are:

- $\text{min} := \left| \min_{(x,y)\in\mathcal{N}_h} u_h(x,y) \right|,$
- $\text{max} := \max_{(x,y)\in\mathcal{N}_h} u_h(x,y) - 1,$
- $\text{min2} := \left(\sum_{(x,y)\in\mathcal{N}_h} (\min\{0, u_h(x,y)\})^2 \right)^{1/2},$
- $\text{max2} := \left(\sum_{(x,y)\in\mathcal{N}_h} (\max\{0, u_h(x,y)-1\})^2 \right)^{1/2},$
- $\text{mino} := \left| \min_{(x,y)\in\mathcal{N}_h\cap\overline{\partial\Omega_N}} u_h(x,y) \right|,$
- $\text{maxo} := \max\{u_h(0,y) - u_h(0,z) : y_0 \le y \le z \le y_{1/2} \text{ or } y_{1/2} \le z \le y \le y_1\},$

  where, denoting by $[\overline{y}_0, \overline{y}_1]$ the interval on the outflow boundary with $u_h(0, y) \ge 0.1$, the point y_0 is such that $\partial_y u_h > 0$ a.e. on $[\overline{y}_0, y_0]$ and $\partial_y u_h(y_0 +) \le 0$. Similarly, $\partial_y u_h < 0$ a.e. on $[y_1, \overline{y}_1]$ and $\partial_y u_h(y_1 -) \ge 0$. Finally, $(0, y_{1/2})$ is the nearest node to $(0, (y_0 + y_1)/2)$. Note that u is non-decreasing on $[\overline{y}_0, 1/2]$ and non-increasing on $[1/2, \overline{y}_1]$ and hence maxo tries to find the largest violation of these monotonicities.

- $\textit{smear} := (d - d_{\text{ref}})/d_{\text{ref}},$

  where d is the sum of the lengths of the two intervals on the outflow boundary with $u_h(0, y) \in [0.1, 0.9]$ and $d_{\text{ref}} = 0.114518$ is the value of d for the interpolation of the reference curve on an equidistant grid with mesh width 1/32 (cf. Figure 2),

- $\textit{width} := (w - w_{\text{ref}})/w_{\text{ref}},$

  where w is the length of the interval on the outflow boundary with $u_h(0, y) \ge 0.1$ and $w_{\text{ref}} = 0.385697$ is the value of w for the interpolation of the reference curve on an equidistant grid with mesh width 1/32.

The measures min and max quantify the size of the largest undershoot or overshoot, respectively. An average value for the undershoots and overshoots is obtained with min2 and max2. The oscillations on the outflow boundary are measured with mino and maxo. The values for smear and width describe the smearing of the layers on the outflow boundary.

The results for the moderate Péclet number case are given in Tables 1–4. It can be seen that all SOLD methods considerably reduce the spurious oscillations of the SUPG solution. However, they also increase the smearing of the layers. Concerning the reduction of the oscillations, the best results are obtained with MH85 on

the simplicial meshes and with dCG91 and BE02 on the quadrilateral mesh. The second best method on the simplicial grids was C93. The edge stabilisation method BE05 gives quite poor results on the regular triangular grids. It becomes much better in comparison with the other methods on the unstructured mesh. The good performance of edge stabilisation methods on unstructured grids was observed already by John and Knobloch (2007). It is noteworthy that the results on Grid 2 are worse than on Grid 1 although the local Péclet numbers are smaller on Grid 2. This shows that the orientation of the edges in Grid 1 is better suited to the direction of the convection in this example. Let us mention that, in all computations, the difference of $u_h(0, 0.5)$ to 1 was less than 1%.

Even in the small local Péclet number case, there is no method that worked satisfactorily in all respects.

Table 1 Results for the computations with moderate local mesh Péclet number, Grid 1

	min	*max*	*min2*	*max2*	*mino*	*maxo*	*smear*	*width*
SUPG	1.068 e–1	8.374 e–2	3.137 e–1	2.544 e–1	3.183 e–2	3.933 e–2	2.225 e–1	7.338 e–2
MH85	2.131 e–12	0.000 e+0	5.189 e–12	0.000 e+0	0.000 e+0	0.000 e+0	6.242 e–1	1.330 e–1
dCG91	8.489 e–3	5.589 e–3	9.316 e–3	8.317 e–3	4.150 e–6	0.000 e+0	8.565 e–1	1.672 e–1
C93	1.247 e–4	3.136 e–4	1.266 e–4	3.209 e–4	0.000 e+0	0.000 e+0	6.591 e–1	1.398 e–1
BE02	3.761 e–3	2.663 e–3	3.915 e–3	3.005 e–3	0.000 e+0	0.000 e+0	8.713 e–1	1.693 e–1
BE05	2.544 e–2	1.604 e–2	6.243 e–2	4.403 e–2	4.367 e–3	7.453 e–3	4.504 e–1	1.084 e–1

Table 2 Results for the computations with moderate local mesh Péclet number, Grid 2

	min	*max*	*min2*	*max2*	*mino*	*maxo*	*smear*	*width*
SUPG	1.242 e–1	1.020 e–1	4.808 e–1	4.229 e–1	4.833 e–2	5.879 e–2	6.661 e–1	1.390 e–1
MH85	7.416 e–13	0.000 e+0	1.888 e–12	0.000 e+0	0.000 e+0	0.000 e+0	1.570 e+0	2.769 e–1
dCG91	1.972 e–2	1.833 e–2	7.519 e–2	8.377 e–2	1.175 e–2	0.000 e+0	1.298 e+0	2.334 e–1
C93	5.792 e–3	2.856 e–3	1.297 e–2	7.815 e–3	1.651 e–3	0.000 e+0	1.464 e+0	2.569 e–1
BE02	1.167 e–2	1.333 e–2	3.930 e–2	4.528 e–2	6.099 e–3	0.000 e+0	1.309 e+0	2.354 e–1
BE05	4.335 e–2	3.003 e–2	1.047 e–1	7.845 e–2	7.449 e–3	0.000 e+0	1.263 e+0	2.279 e–1

Table 3 Results for the computations with moderate local mesh Péclet number, Grid 3

	min	*max*	*min2*	*max2*	*mino*	*maxo*	*smear*	*width*
SUPG	7.204 e–2	9.425 e–2	3.452 e–1	3.639 e–1	4.712 e–2	4.682 e–2	2.705 e–1	8.894 e–2
MH85	1.528 e–12	0.000 e+0	3.802 e–12	0.000 e+0	0.000 e+0	0.000 e+0	9.717 e–1	1.877 e–1
dCG91	5.408 e–2	3.589 e–2	9.850 e–2	7.845 e–2	4.952 e–3	0.000 e+0	9.097 e–1	1.877 e–1
C93	2.754 e–2	3.273 e–2	5.494 e–2	5.519 e–2	2.188 e–3	0.000 e+0	6.914 e–1	1.553 e–1
BE02	4.047 e–2	2.966 e–2	6.832 e–2	5.479 e–2	1.688 e–3	0.000 e+0	9.455 e–1	1.924 e–1
BE05	3.111 e–2	2.905 e–2	7.437 e–2	6.821 e–2	6.212 e–3	6.071 e–3	7.072 e–1	1.569 e–1

Table 4 Results for the computations with moderate local mesh Péclet number, Grid 4

	min	*max*	*min2*	*max2*	*mino*	*maxo*	*smear*	*width*
SUPG	1.316 e–1	1.026 e–1	4.205 e–1	3.311 e–1	4.235 e–2	5.191 e–2	3.544 e–1	9.283 e–2
dCG91	1.244 e–2	7.865 e–3	2.381 e–2	1.477 e–2	4.049 e–4	0.000 e+0	9.936 e–1	1.906 e–1
C93	3.311 e–2	2.908 e–2	5.992 e–2	4.414 e–2	1.299 e–5	0.000 e+0	7.823 e–1	1.535 e–1
BE02	1.351 e–2	8.321 e–3	2.267 e–2	1.180 e–2	5.280 e–8	0.000 e+0	1.022 e+0	1.958 e–1

Remark 1: *The results in Tables 1–4 also show that the quality of the solution on the outflow boundary is often better than of the solution inside* Ω *and hence the outflow profile cannot be used as the only measure for an assessment of the considered numerical methods. For the Galerkin discretisation with small* ε*, it can even happen that the inflow profile is almost exactly reproduced on the outflow boundary whereas the solution wildly oscillates inside* Ω*.*

4.2 High local mesh Péclet numbers

We consider the same example as before, however, with the diffusion parameter $\varepsilon = 10^{-8}$. The regular Grids 1, 2 and 4 from Figure 3 are used with edges (legs of the triangles) of length 1/64. The number of degrees of freedom for the P_1, resp. Q_1, discretisation is 4225 (including Dirichlet nodes). The unstructured grid, which was used in the high local mesh Péclet number computations has 1721 nodes and is presented in Figure 4. The largest local mesh Péclet numbers are around 7.7×10^5 for Grid 2, 1.5×10^6 for Grid 1 and Grid 4 and 2.1×10^6 for Grid 5.

Concerning the oscillations, the same measures are used as in the moderate local Péclet number case. The smearing of the layers will be evaluated by means of graphs of the discrete solutions on the outflow boundary. Thus, the measures do not need a reference solution.

Figure 4 Unstructured Grid 5 for the high local Péclet number case

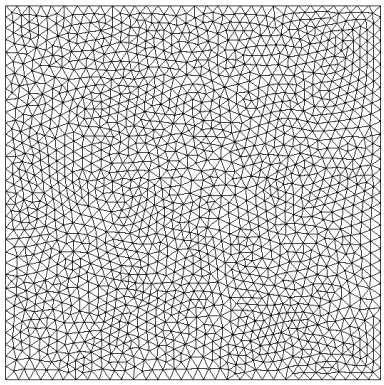

The results concerning the spurious oscillations are collected in Tables 5–8. All SOLD methods give again much better results than the SUPG method. Only on the regular Grids 1 and 2, the fixed-point iterations for solving the non-linear problem of BE05 did not converge (100,000 iterations). On the triangular grids, MH85 was again the best

method. Among the other methods, there is no really a best one. BE02 is slightly better than the other ones on Grid 1 and C93 on Grid 2. On the unstructured Grid 5, the edge stabilisation method BE05 is the second best after MH85. We think that the good performance of MH85 on Grid 3 (with $\varepsilon = 10^{-4}$) and Grid 5 might be caused by the fact that these grids possess only acute triangles. On the quadrilateral Grid 4, all SOLD methods give similar results. Note that the amount of the spurious oscillations is not much different in comparison with the moderate local Péclet number case.

Table 5 Results for the computations with high local mesh Péclet number, Grid 1

	min	*max*	*min2*	*max2*	*mino*	*maxo*
SUPG	1.551 e–1	1.353 e–1	6.602 e–1	5.734 e–1	5.533 e–2	7.004 e–2
MH85	1.176 e–12	6.160 e–13	4.627 e–12	1.406 e–12	3.414 e–13	0.000 e+0
dCG91	5.579 e–3	3.979 e–3	8.559 e–3	6.268 e–3	5.266 e–6	0.000 e+0
C93	5.004 e–3	1.681 e–4	7.299 e–3	1.723 e–4	2.784 e–6	1.602 e–6
BE02	2.198 e–3	1.567 e–3	2.933 e–3	2.119 e–3	5.675 e–8	0.000 e+0
BE05	No convergence					

Table 6 Results for the computations with high local mesh Péclet number, Grid 2

	min	*max*	*min2*	*max2*	*mino*	*maxo*
SUPG	1.655 e–1	1.467 e–1	8.311 e–1	7.438 e–1	6.313 e–2	6.815 e–2
MH85	1.086 e–12	5.294 e–13	3.868 e–12	1.296 e–12	2.500 e–13	0.000 e+0
dCG91	1.405 e–2	1.174 e–2	7.014 e–2	6.853 e–2	7.660 e–3	3.375 e–3
C93	3.948 e–3	1.567 e–3	9.394 e–3	3.714 e–3	4.840 e–4	6.758 e–4
BE02	7.501 e–3	8.482 e–3	3.405 e–2	3.152 e–2	3.951 e–3	9.976 e–4
BE05	No convergence					

Table 7 Results for the computations with high local mesh Péclet number, Grid 4

	min	*max*	*min2*	*max2*	*mino*	*maxo*
SUPG	1.868 e–1	1.642 e–1	8.126 e–1	6.755 e–1	6.618 e–2	6.740 e–2
dCG91	2.861 e–2	2.562 e–2	5.910 e–2	4.747 e–2	1.330 e–4	1.832 e–5
C93	3.898 e–2	3.464 e–2	7.993 e–2	6.243 e–2	7.491 e–6	2.859 e–5
BE02	2.961 e–2	2.740 e–2	5.932 e–2	4.854 e–2	5.965 e–6	1.424 e–5

Table 8 Results for the computations with high local mesh Péclet number, Grid 5

	min	*max*	*min2*	*max2*	*mino*	*maxo*
SUPG	1.156 e–1	9.801 e–2	5.591 e–1	4.947 e–1	7.953 e–2	7.639 e–2
MH85	9.530 e–13	0.000 e+0	2.839 e–12	0.000 e+0	2.029 e–13	0.000 e+0
dCG91	6.264 e–2	7.172 e–2	9.784 e–2	9.648 e–2	6.206 e–3	0.000 e+0
C93	4.470 e–2	4.347 e–2	5.771 e–2	6.197 e–2	2.936 e–4	0.000 e+0
BE02	4.974 e–2	5.225 e–2	6.785 e–2	6.691 e–2	1.995 e–3	0.000 e+0
BE05	3.528 e–2	3.122 e–2	5.767 e–2	5.429 e–2	4.108 e–3	2.622 e–3

Parts of the outflow profiles for selected methods are presented in Figures 5–8. The improvement in comparison with the SUPG solution concerning the spurious oscillations is clearly visible. Likewise, the smearing of the layers in the solutions computed with the SOLD methods can be seen. The smearing is more or less the same for all SOLD methods. Often, the curves are on top of each other. All layers (including the SUPG solution) are extremely smeared on Grid 2. This is a further hint that this grid is less suited for the present example than the other ones. The reason for the stronger smearing of the layers on Grid 5 in comparison with Grids 1 and 4 is the considerably smaller number of degrees of freedom on Grid 5.

The method MH85 practically removes the spurious oscillations in the high local Péclet number computations. The spurious oscillations of the other methods are still not negligible. In addition, all SOLD methods lead to a smearing of the layers.

Figure 5 Solution at the lower part of the outflow boundary for the high local Péclet number case, Grid 1

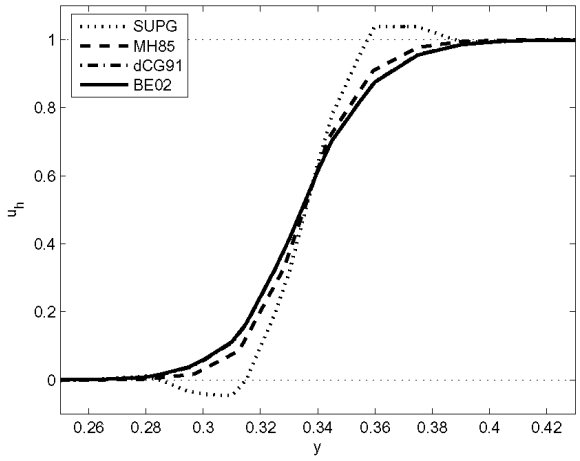

Figure 6 Solution at the lower part of the outflow boundary for the high local Péclet number case, Grid 2

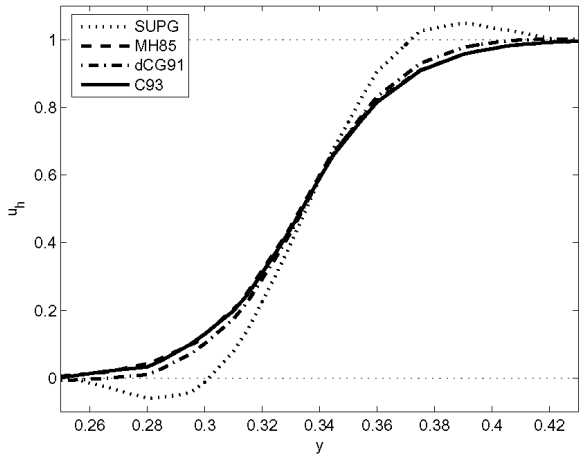

Figure 7 Solution at the lower part of the outflow boundary for the high local Péclet number case, Grid 4

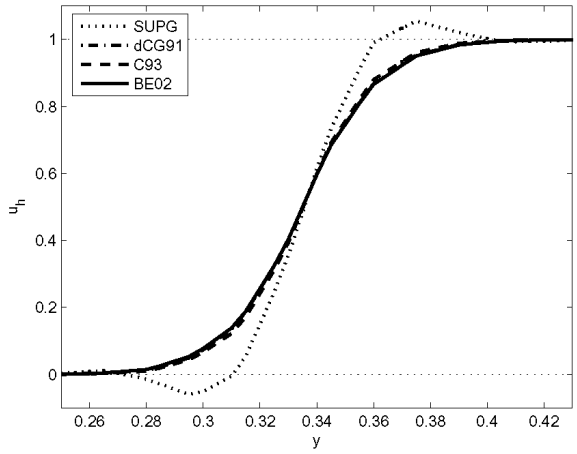

Figure 8 Solution at the lower part of the outflow boundary for the high local Péclet number case, Grid 5

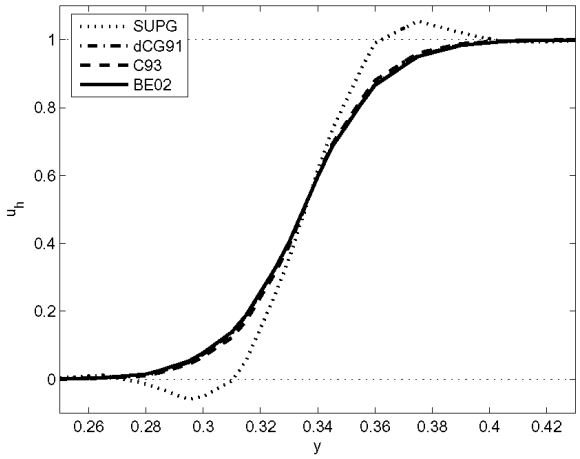

5 Conclusions

The present numerical studies support an observation by John and Knobloch (2007): if the upwind method MH85 can be used, then it is the best method. The edge stabilisation method BE05 worked only properly on the unstructured grids with acute triangles. The differences among the other SOLD methods were small. On the one hand, their results are clearly better than the results of the SUPG method, but on the other hand, the remaining spurious oscillations are still not tolerable in many applications. Combining the results of John and Knobloch (2007) and the present study, one has to conclude that the SOLD methods are still far away from being able to solve convection-dominated problems successfully.

Acknowledgement

The research of Petr Knobloch is a part of the project MSM 0021620839 financed by MSMT and it was partly supported by the Grant Agency of the Academy of Sciences of the Czech Republic under the Grant No. IAA100190505.

References

Brooks, A.N. and Hughes, T.J.R. (1982) 'Streamline upwind/Petrov–Galerkin formulations for convection dominated flows with particular emphasis on the incompressible Navier-Stokes equations', *Comput. Methods Appl. Mech. Eng.*, Vol. 32, pp.199–259.

Burman, E. and Ern, A. (2002) 'Nonlinear diffusion and discrete maximum principle for stabilized Galerkin approximations of the convection–diffusion–reaction equation', *Comput. Methods Appl. Mech. Eng*., Vol. 191, pp.3833–3855.

Burman, E. and Ern, A. (2005) 'Stabilized Galerkin approximation of convection–diffusion–reaction equations: discrete maximum principle and convergence', *Math. Comput*., Vol. 74, pp.1637–1652.

Ciarlet, P.G. (1991) 'Basic error estimates for elliptic problems', in Ciarlet, P.G. and Lions, J.L. (Eds.): *Handbook of Numerical Analysis*, Vol. 2 – Finite Element Methods (pt. 1), North Holland, Amsterdam, pp.17–351.

Codina, R. (1993) 'A discontinuity-capturing crosswind-dissipation for the finite element solution of the convection–diffusion equation', *Comput. Methods Appl. Mech. Eng*., Vol. 110, pp.325–342.

do Carmo, E.G.D. and Galeão, A.C. (1991) 'Feedback Petrov–Galerkin methods for convection-dominated problems', *Comput. Methods Appl. Mech. Eng*., Vol. 88, pp.1–16.

Dolejší, V. (1998) 'Anisotropic mesh adaptation for finite volume and finite element methods on triangular meshes', *Comput. Visual. Sci*., Vol. 1, pp.165–178.

Hughes, T.J.R., Franca, L.P. and Hulbert, G.M. (1989) 'A new finite element formulation for computational fluid dynamics. VIII. The Galerkin/least-squares method for advective–diffusive equations', *Comput. Methods Appl. Mech. Eng*., Vol. 73, pp.173–189.

John, V. and Knobloch, P. (2007) 'On spurious oscillations at layers diminishing (SOLD) methods for convection–diffusion equations: part I – a review', *Comput. Methods Appl. Mech. Eng*., Vol. 196, pp.2197–2215.

John, V. and Matthies, G. (2004) 'MooNMD – a program package based on mapped finite element methods', *Comput. Visual. Sci*., Vol. 6, pp.163–170.

Knobloch, P. (2006) 'Improvements of the Mizukami–Hughes method for convection–diffusion equations', *Comput. Methods Appl. Mech. Eng*., Vol. 196, pp.579–594.

Knopp, T., Lube, G. and Rapin, G. (2002) 'Stabilized finite element methods with shock capturing for advection–diffusion problems', *Comput. Methods Appl. Mech. Eng*., Vol. 191, pp.2997–3013.

Mizukami, A. and Hughes, T.J.R. (1985) 'A Petrov–Galerkin finite element method for convection-dominated flows: an accurate upwinding technique for satisfying the maximum principle', *Comput. Methods Appl. Mech. Eng*., Vol. 50, pp.181–193.

Roos, H-G., Stynes, M. and Tobiska, L. (1996) *Numerical Methods for Singularly Perturbed Differential Equations. Convection–Diffusion and Flow Problems*, Springer-Verlag, Berlin.

Tabata, M. (1977) 'A finite element approximation corresponding to the upwind finite differencing', *Mem. Numer. Math*., Vol. 4, pp.47–63.